Multicenter Study of Temporal Changes and Prognostic Value of a CT Visual Severity Score in Hospitalized Patients With Coronavirus Disease (COVID-19)

Xiaofeng Wang, PhD[1,2,3], Xingxing Hu, MD[4], Weijun Tan, MD[5], Peter Mazzone, MD[2,3], Eduardo Mireles-Cabodevila, MD[2,3], Xiaozhen Han, MS[1], Pingyue Huang, MD[6], Weihua Hu, MD[7], Raed Dweik, MD[2,3], Zhenshun Cheng, MD[4,8]

Cardiothoracic Imaging · Original Research

Keywords

change points, complications, COVID-19, prediction, series CT

X. Wang, X. Hu, and W. Tan contributed equally to this work.

Submitted: Jun 7, 2020
Revision requested: Jun 19, 2020
Revision received: Jul 13, 2020
Accepted: Aug 7, 2020
First published online: Sep 9, 2020

The authors declare that they have no disclosures relevant to the subject matter of this article.

Supported by the Key Project for Anti-2019 Novel Coronavirus Pneumonia program of the National Key Research and Development Program of China (grant 2020YFC0845500).

An electronic supplement is available online at doi.org/10.2214/AJR.20.24044.

BACKGROUND. Chest CT findings have the potential to guide treatment of hospitalized patients with coronavirus disease (COVID-19).

OBJECTIVE. The purpose of this study was to assess a CT visual severity score in hospitalized patients with COVID-19, with attention to temporal changes in the score and the role of the score in a model for predicting in-hospital complications.

METHODS. This retrospective study included 161 inpatients with COVID-19 from three hospitals in China who underwent serial chest CT scans during hospitalization. CT examinations were evaluated using a visual severity scoring system. The temporal pattern of the CT visual severity score across serial CT examinations during hospitalization was characterized using a generalized spline regression model. A prognostic model to predict major complications, including in-hospital mortality, was created using the CT visual severity score and clinical variables. External model validation was evaluated by two independent radiologists in a cohort of 135 patients from a different hospital.

RESULTS. The cohort included 91 survivors with nonsevere disease, 55 survivors with severe disease, and 15 patients who died during hospitalization. Median CT visual lung severity score in the first week of hospitalization was 2.0 in survivors with nonsevere disease, 4.0 in survivors with severe disease, and 11.0 in nonsurvivors. CT visual severity score peaked approximately 9 and 12 days after symptom onset in survivors with nonsevere and severe disease, respectively, and progressively decreased in subsequent hospitalization weeks in both groups. In the prognostic model, in-hospital complications were independently associated with a severe CT score (odds ratio [OR], 31.28), moderate CT score (OR, 5.86), age (OR, 1.09 per 1-year increase), and lymphocyte count (OR, 0.03 per 1×10^9/L increase). In the validation cohort, the two readers achieved C-index values of 0.92–0.95, accuracy of 85.2–86.7%, sensitivity of 70.7–75.6%, and specificity of 91.4–91.5% for predicting in-hospital complications.

CONCLUSION. A CT visual severity score is associated with clinical disease severity and evolves in a characteristic fashion during hospitalization for COVID-19. A prognostic model based on the CT visual severity score and clinical variables shows strong performance in predicting in-hospital complications.

CLINICAL IMPACT. The prognostic model using the CT visual severity score may help identify patients at highest risk of poor outcomes and guide early intervention.

A novel coronavirus disease (COVID-19), caused by severe acute respiratory syndrome coronavirus 2 (SARS-CoV-2), was identified as the cause of a cluster of pneumonia cases in Wuhan, China, at the end of 2019 [1]. It quickly spread throughout China, and an increasing number of cases in other countries followed. In March 2020, the WHO declared the COVID-19 outbreak a global pandemic.

The clinical characteristics of COVID-19 have been reported by several studies [2–5]. The main clinical manifestations include fever, cough, shortness of breath, fatigue, and

[1]Department of Quantitative Health Sciences, Lerner Research Institute, Cleveland Clinic, Cleveland, OH.

[2]Department of Pulmonary Medicine, Respiratory Institute, Cleveland Clinic, Cleveland, OH.

[3]Department of Critical Care Medicine, Respiratory Institute, Cleveland Clinic, Cleveland, OH.

[4]Department of Pulmonary and Critical Care Medicine, Zhongnan Hospital of Wuhan University, Wuhan, Hubei 430071, China. Address correspondence to Z. Cheng (chzs1990@163.com).

[5]Department of Pulmonary and Critical Care Medicine, Central Hospital of Wuhan, Tongji Medical College, Huazhong University of Science and Technology, Wuhan, China.

[6]Department of Thoracic Surgery, Jingzhou Chest Hospital, Jingzhou, China.

[7]Department of Pulmonary Medicine, The First People's Hospital of Jingzhou, Yangtze University, Jingzhou, China.

[8]Wuhan Research Center for Infectious Diseases and Cancer, Chinese Academy of Medical Sciences, Beijing, China.

doi.org/10.2214/AJR.20.24044

AJR 2021; 217:83–92

ISSN-L 0361–803X/21/2171–83

dyspnea. In a large epidemiologic study of 1099 patients, Guan et al. [5] compared patients with severe and nonsevere disease according to the degree of severity at the time of hospital admission. Most patients showed lymphopenia and elevated levels of liver enzymes, creatine kinase, and D-dimer. Patients with severe disease had more prominent laboratory abnormalities (i.e., leukopenia, lymphopenia, thrombocytopenia) and an increased risk of developing organ dysfunction, including acute respiratory distress syndrome (ARDS) and acute kidney injury (AKI).

CT has been reported as an important tool in assisting the diagnosis and treatment of patients with COVID-19 [6–9]. The imaging features of COVID-19 pneumonia are diverse, ranging from normal appearance to diffuse changes in the lungs. Moreover, disease progression can be characterized by CT. For example, Shi et al. [7] described the CT findings from 81 patients across different time points during the disease course. Pan et al. [8] and Wang et al. [9] investigated the time course of lung changes on chest CT during recovery. However, the association of CT findings with clinical disease severity and the evolution of these findings have not been well described. In this study, we explored a CT visual severity score in hospitalized patients with COVID-19, with attention to temporal changes in the score and the role of the score in a model for predicting in-hospital complications.

HIGHLIGHTS

Key Finding

- *Median CT visual lung severity score in the first hospitalization week was 2.0–4.0 in discharged patients versus 11.0 in those who died. A prognostic model for predicting in-hospital complications using the CT score showed strong performance in an external validation cohort (C-index, 0.92–0.95; accuracy, 85.2–86.7%; sensitivity, 70.7–75.6%; specificity, 91.4–91.5%).*

Importance

- *A prognostic model using the CT visual severity score and clinical variables may identify patients at highest risk of poor outcomes and guide early intervention.*

Methods

Study Design

We conducted a multicenter retrospective cohort study in Hubei Province, China. The study was approved by the ethics committee in each participating hospital. Written informed consent was waived because of the observational nature of the study and the epidemic of COVID-19 as an emergency public health event.

We included patients with confirmed COVID-19 pneumonia who were admitted to one of three hospitals in Hubei, all designated for COVID-19, and who underwent at least two chest CT scans after admission. The COVID-19 diagnosis at the three hospitals was initially based on the criteria published by WHO on January 28, 2020 [1], and all cases were later confirmed by real-time reverse-transcriptase polymerase chain reaction analysis of throat swab specimens according to a previously published protocol [2, 4]. Patients with a confirmed diagnosis were treated with effective isolation and protective conditions in the hospitals, and patients with severe and critical disease were admitted to the emergency department or ICU ward. All patients underwent initial laboratory testing, including complete blood count, coagulation profile, renal and liver function, creatine kinase, lactate dehydrogenase, and electrolytes. All patients' vital signs (body temperature, heart rate, blood pressure, and respiratory rate) were monitored during their hospitalization. Patients at all centers received treatment that followed the guidelines established by Jin et al. [10]. All of the patients received antibacterial agents. The use of antiviral therapy and methylprednisolone varied depending on disease severity. For patients with severe disease, continuous renal replacement therapy was applied if acute renal impairment or failure occurred. Invasive mechanical ventilation was administered to patients with hypoxic respiratory failure and ARDS. Extracorporeal membrane oxygenation support was used for patients with refractory hypoxemia that was difficult to correct by prone positioning and protective lung ventilation. More detailed treatment strategies performed at these centers are described by Zhang et al. [11].

To be discharged, patients needed to satisfy all of the following four criteria: afebrile for more than 3 days, two consecutive negative results on reverse-transcriptase polymerase chain reaction tests conducted at least 24 hours apart, significantly improved respiratory symptoms, and improvement in the radiologic abnormalities on chest radiograph or CT.

Clinical Data Collection and CT Image Acquisition

Demographic, clinical, laboratory, and outcome data were extracted from electronic medical records using a standardized data collection form, which was a modified version of the WHO and International Severe Acute Respiratory and Emerging Infection Consortium case record form for severe acute respiratory infections [12]. Data were extracted from the time of patients' initial hospital admission until either hospital discharge or mortality. This extraction was performed by two physicians (X.H., a pulmonologist with 5 years of experience, and W.T., a pulmonologist with 15 years of experience). A third physician (Z.C., a pulmonologist with 25 years of experience) adjudicated any difference in interpretation between the two primary reviewers.

Cases of COVID-19 were classified as severe or nonsevere at the time of hospital admission using the American Thoracic Society guidelines for community-acquired pneumonia [5, 13]. Patients were classified as having severe disease if they had any of the following: dyspnea, respiratory frequency of 30 breaths/min or more, blood oxygen saturation of 93% or lower, Pa_{O_2}:Fi_{O_2} ratio of less than 300, or an increase in lung infiltrates of over 50% within a period of 24–48 hours. Patients with severe disease generally required supplemental oxygen, although this was not a criterion for the classification.

Chest CT scans were performed with a single inspiratory phase using an MDCT scanner (Somatom Definition AS, Siemens Healthineers; Somatom Definition Flash, Siemens Healthineers; or GE BrightSpeed 16, GE Healthcare). Patients were instructed on breath-holding to minimize motion artifacts. All CT scans were obtained with the patient in the supine position during a single breath-hold without IV contrast material. The tube voltage

was 120 kV for all scans. The tube current–exposure time product and CT doses varied across scans. Automatic exposure control technology was used to automatically adjust the tube current for each patient.

CT Image Review and Visual Severity Scores

Two physicians at Zhongnan Hospital of Wuhan University (Z.C. and X.H.), Central Hospital of Wuhan (W.T. and a nonauthor radiologist with 15 years), and Jingzhou Chest Hospital (P.H., a radiologist with 20 years, and a nonauthor radiologist with 15 years) scored the CT images and were unaware of patients' clinical status. As training before the evaluation, the investigators reviewed CT images from a group of eight patients with severity scores ranging from none to severe. After initial independent evaluations, the two physicians at each hospital discussed any disagreements to reach consensus.

Pulmonary disease severity on CT scans was assessed visually. Each scan was assigned to one of the following categories: no ground-glass opacity (GGO) or consolidation, GGO only, consolidation only, or both GGO and consolidation. GGO was defined as an area of haziness with increased attenuation that did not obscure the underlying vascular markings. Consolidation was defined as opacity obscuring the underlying vascular markings. Each scan was also assessed for the presence of a peripheral distribution of opacification, linear opacities, or crazy paving pattern. Each lobe branching off the main bronchus (three on the right, two on the left) was assessed for involvement. A visual severity score was assigned to each lobe using four categories of lobe involvement on the basis of GGO and consolidation: 0, none (0% involvement); 1, mild (< 50% involvement); 2, moderate (50–75% involvement); and 3, severe (> 75% involvement). An overall CT visual severity score was reached by summing the scores for the five lobes (possible range for summed scores, 0–15).

Outcome Measures

The primary measured outcome for this study was a composite endpoint of major COVID-19–associated complications. Major complications included ARDS, acute cardiac injury, arrhythmia, septic shock, AKI, liver dysfunction, secondary infection, and in-hospital mortality (defined as death from any cause before discharge). ARDS was diagnosed according to the Berlin definition [14], and AKI was diagnosed according to the Kidney Disease Improving Global Outcomes clinical practice guidelines [15]. Acute cardiac injury was diagnosed if serum levels of cardiac biomarkers (i.e., troponin I) were above the 99th percentile upper reference limit or if new abnormalities appeared on ECG and echocardiography [2]. Sepsis and septic shock were defined according to the "Third International Consensus Definitions for Sepsis and Septic Shock" published in 2016 [16]. Liver dysfunction was diagnosed if alanine aminotransferase and aspartate aminotransferase increased during the course of disease [17, 18]. Secondary infection was diagnosed if the patients showed clinical symptoms or signs of nosocomial pneumonia or bacteremia and had a culture that was positive for a new pathogen from a lower respiratory tract specimen (including sputum, transtracheal aspirates, or bronchoalveolar lavage fluid) or from blood samples taken 48 hours or more after admission [2].

Statistical Analysis

The study variables were evaluated using the sample median with interquartile range (IQR) or the number with proportion. The study sample was divided into three groups on the basis of disease severity at hospital admission and survival status: survivors with nonsevere disease, survivors with severe disease, and nonsurvivors. The three groups were compared in terms of clinical features on admission. Categoric variables were compared between groups using the Pearson chi-square test or Fisher exact test, whereas continuous variables were compared using the nonparametric Kruskal-Wallis test. The analysis of interreader agreement was conducted using weighted kappa coefficients.

The findings on lung CT were compared among four groups defined by the amount of time between the onset of symptoms and CT scan: week 1 (e.g., scans performed within the first week after symptom onset), week 2, week 3, and week 4 or later. Nonsurvivors with severe disease only had scans available in weeks 1 and 2; nonsurvivors were typically critically ill patients who had to use noninvasive or invasive ventilators and did not undergo additional CT scans after 2 weeks of hospitalization. If a patient had multiple CT scans within one of these four time periods, the first of these scans was used for the analysis.

To investigate the nonlinear temporal evolution of CT findings, we built generalized additive models with penalized splines [19], in which the expected value of CT score is related to the scan time period via a nonparametric smooth function. We estimated the nonlinear disease progression curves by considering the time of CT as a continuous predictor. Nonsurvivors were not considered in this analysis given the lack of data. Nonparametric analysis of covariance was conducted to test the parallelism of the nonlinear temporal functions between the groups of survivors with nonsevere and severe disease [20]. A change point detection analysis [21] was performed to estimate the time of peak severity for the three groups.

Univariable and multivariable logistic regression analyses were performed to assess the association between the risk factors and patient outcome. To avoid overfitting, four variables were chosen for the multivariable prediction model on the basis of previous research findings and clinical constraints. In the multivariable model, the CT visual severity score was classified as none or mild (score 0–5), moderate (score 6–10), or severe (score 11–15). Correlation analysis of the predictors was conducted to avoid the multicollinearity in a regression model. Following the guidelines of the Transparent Reporting of a multivariable prediction model for Individual Prognosis or Diagnosis (TRIPOD) statement [22], bootstrap internal validation was conducted for the model, including an evaluation of the model's discriminative ability and calibration [23]. An online risk calculator was created based on the model [24]. The source code for this online risk calculator is available in the Supplemental Methods, which can be viewed in the *AJR* electronic supplement to this article, available at www.ajronline.org.

External validation was then performed using an independent external cohort to evaluate the overall accuracy of the model. For this external cohort, 135 hospitalized patients with COVID-19 were retrospectively identified from a fourth hospital designated for COVID-19 in Hubei during the same time period as the cohort from the other three hospitals. Data were collected for these pa-

TABLE 1: Clinical Characteristics of the Study Patients According to Coronavirus Disease (COVID-19) Severity and Survival

Characteristic	Total Patients (*n* = 161)	Survivors With Nonsevere Disease (*n* = 91)	Survivors With Severe Disease (*n* = 55)	Nonsurvivors (*n* = 15)	*p*[a]
Age (y)	42.0 (33.0–57.0)	37.0 (30.5–45.5)	53.0 (39.0–62.5)	72.0 (64.5–74.5)	< .001
Sex					.02
Female	72 (44.7)	49 (53.8)	20 (36.4)	3 (20.0)	
Male	89 (55.3)	42 (46.2)	35 (63.6)	12 (80.0)	
Weight (kg)	62.0 (53.3–70.0)	60.0 (52.0–70.0)	65.0 (59.5–73.0)	60.0 (60.0–64.3)	.07
Medical staff	40 (24.8)	28 (30.8)	12 (21.8)	0 (0)	.02
Comorbidity					
Hypertension	21 (13.0)	2 (2.2)	10 (18.2)	9 (60.0)	< .001
Diabetes	6 (3.7)	0 (0)	5 (9.1)	1 (6.7)	.007
CVD	4 (2.5)	0 (0)	2 (3.6)	2 (13.3)	.008
CKD	2 (1.2)	0 (0)	0 (0)	2 (13.3)	.008
Immunodeficiency	5 (3.1)	1 (1.1)	1 (1.8)	3 (20.0)	.006
Signs and symptoms					
Fever	136 (84.5)	73 (80.2)	49 (89.1)	14 (93.3)	.28
Muscular soreness	47 (29.2)	25 (27.5)	18 (32.7)	4 (26.7)	.81
Dry cough	78 (48.4)	45 (49.5)	28 (50.9)	5 (33.3)	.46
Fatigue	59 (36.6)	30 (33.0)	17 (30.9)	12 (80.0)	.001
Diarrhea	10 (6.2)	3 (3.3)	4 (7.3)	3 (20.0)	.05
Emesis	3 (1.9)	1 (1.1)	1 (1.8)	1 (6.7)	.29
Expectoration	30 (18.6)	14 (15.4)	12 (21.8)	4 (26.7)	.40
Hemoptysis	5 (3.1)	2 (2.2)	2 (3.6)	1 (6.7)	.37
Headache	14 (8.7)	7 (7.7)	6 (10.9)	1 (6.7)	.83
Rhinorrhea	5 (3.1)	4 (4.4)	1 (1.8)	0 (0)	.79
Dyspnea	9 (5.6)	1 (1.1)	1 (1.8)	7 (46.7)	< .001
Nasal congestion	3 (1.9)	3 (3.3)	0 (0)	0 (0)	.47
Chest tightness	28 (17.4)	14 (15.4)	12 (21.8)	2 (13.3)	.64
Temperature (°C)	37.50 (36.80–38.20)	37.40 (36.75–38.20)	37.90 (37.15–38.30)	37.20 (36.40–38.20)	.16
SBP (mm Hg)	120.00 (117.00–130.00)	120.00 (116.00–126.50)	123.00 (116.50–130.00)	130.00 (126.00–137.50)	.004
DBP (mm Hg)	75.00 (70.00–80.00)	75.00 (70.00–80.00)	73.00 (69.00–80.00)	80.00 (77.00–84.50)	.09
HR (beats/min)	87.00 (79.00–98.00)	85.00 (78.50–96.00)	90.00 (78.00–101.50)	89.00 (82.00–99.00)	.32
RR (breaths/min)	20.00 (18.00–20.00)	20.00 (18.00–20.00)	20.00 (19.00–22.00)	22.00 (20.00–25.50)	< .001

Note—Data are the median (interquartile range) or number of patients (percentage) unless otherwise indicated. CVD = cardiovascular disease, CKD = chronic kidney disease, SBP = systolic blood pressure, DBP = diastolic blood pressure, HR = heart rate, RR = respiratory rate.

[a]Values compare patients with nonsevere disease, survivors with severe disease, and nonsurvivors with severe disease and are calculated from chi-square test, Fisher exact test, or Kruskal-Wallis test.

tients using the same method as described for the internal cohort. Two readers (W.H., a pulmonologist with 20 years of experience, and a nonauthor radiologist with 20 years) independently reviewed these patients' CT images, which were obtained at the time of hospital admission, and provided a single CT visual severity level: none or mild, < 50% involvement; moderate, 50–75% involvement; or severe, > 75% involvement.

All analyses were performed using the R software program (version 3.6.3, R Foundation for Statistical Computing). The level of statistical significance was set at $p < .05$ (two-tailed).

Results

Clinical Characteristics and Laboratory Findings

A total of 161 hospitalized patients (55.3% [89/161] men and 44.7% [72/161] women) who underwent at least two CT scans following admission were included (Table 1). The median age was 42.0 years (IQR, 33.0–57.0 years). The most common symptoms on admission were fever (84.5%) and cough (48.4%); vomiting (1.9%) and diarrhea (6.2%) were uncommon.

On admission, COVID-19 was nonsevere in 56.5% of patients (91/161) and severe in 43.5% (70/161). Of patients with severe dis-

TABLE 2: Laboratory Test Results for Patients With Coronavirus Disease (COVID-19) on Admission to Hospital, Stratified by Patient Group

Test	Normal Values	Total Patients (*n* = 161)	Survivors With Nonsevere Disease (*n* = 91)	Survivors With Severe Disease (*n* = 55)	Nonsurvivors (*n* = 15)	*p*[a]
WBC count (× 10^9/L)	3.5–9.5	4.38 (3.39–5.62)	4.22 (3.38–5.11)	4.40 (3.29–5.96)	6.77 (4.07–7.91)	.01
> 10		5 (3.1)	0 (0.0)	3 (5.5)	2 (13.3)	.009
< 4		65 (40.4)	41 (45.1)	21 (38.2)	3 (20.0)	.17
Neutrophil count (× 10^9/L)	1.8–6.3	2.85 (2.05–3.90)	2.52 (1.87–3.49)	3.13 (2.07–4.31)	6.17 (3.23–6.93)	< .001
Lymphocyte count (× 10^9/L)	1.1–3.2	0.98 (0.68–1.27)	1.07 (0.89–1.39)	0.83 (0.64–1.18)	0.44 (0.38–0.77)	< .001
< 1.5		142 (88.2)	76 (83.5)	52 (94.5)	14 (93.3)	.09
Monocyte count (× 10^9/L)	0.1–0.6	0.39 (0.26–0.49)	0.41 (0.27–0.50)	0.36 (0.26–0.50)	0.21 (0.18–0.42)	.04
Platelet count (× 10^9/L)	125–350	166.0 (129.0–197.0)	164.0 (131.0–192.0)	178.0 (134.0–202.0)	104.0 (90.0–172.5)	.05
< 150		60 (37.3)	34 (37.4)	17 (30.9)	9 (60.0)	.12
Procalcitonin (ng/mL)	< 0.05	0.030 (0.025–0.090)	0.025 (0.025–0.050)	0.055 (0.025–0.092)	0.485 (0.218–1.377)	< .001
≥ 0.05		61 (37.9)	22 (24.2)	27 (49.1)	12 (80.0)	< .001
D-Dimer (mg/L)	0–0.5	0.22 (0.13–0.55)	0.17 (0.12–0.30)	0.28 (0.16–0.64)	1.12 (0.43–9.29)	< .001
≥ 0.5		35 (21.7)	11 (12.1)	14 (25.5)	10 (66.7)	< .001
Prothrombin time (s)	9.4–12.5	12.30 (11.55–13.05)	12.35 (11.50–12.80)	12.45 (11.60–13.20)	12.30 (11.75–13.60)	.56
ALT (U/L)	9–50	24.5 (17.7–35.3)	22.0 (16.0–29.8)	28.0 (20.8–42.5)	22.5 (17.1–53.0)	.03
AST (U/L)	15–40	22.0 (16.0–30.8)	20.6 (15.0–26.5)	24.0 (16.0–37.5)	29.5 (22.0–40.9)	.03
Total bilirubin (μmol/L)	5–21	9.3 (7.2–11.8)	8.9 (7.1–11.5)	9.4 (7.3–11.8)	13.2 (10.1–16.5)	.007
BUN (mmol/L)	2.8–7.6	4.04 (3.27–4.99)	3.81 (3.07–4.42)	4.20 (3.33–5.04)	6.80 (4.94–10.53)	< .001
Creatinine (μmol/L)	64–104	69.2 (56.2–83.3)	66.7 (53.1–79.9)	71.5 (60.2–82.1)	88.1 (63.7–107.5)	.009
Creatine kinase (U/L)	< 171	74.2 (47.0–130.0)	70.0 (43.6–117.0)	87.0 (60.0–136.0)	106.0 (54.0–209.5)	.12
Creatine kinase-MB (U/L)	< 25	10.7 (8.0–14.0)	10.0 (8.0–13.3)	10.0 (8.0–13.6)	19.4 (11.5–25.0)	.02
LDH (U/L)	125–243	191.0 (152.8–325.0)	172.0 (139.5–210.5)	242.0 (164.0–343.0)	452.0 (376.5–633.5)	< .001
High-sensitivity troponin I (pg/mL)	< 26.2	9.90 (3.20–20.00)	8.00 (3.00–10.00)	6.70 (3.00–15.60)	22.80 (8.50–58.20)	.007

Note—Data are the median (interquartile range) or number of patients (percentage) unless otherwise indicated. ALT = alanine aminotransferase, AST = aspartate aminotransferase, BUN = blood urea nitrogen, MB = myocardial band, LDH = lactate dehydrogenase.
[a]Values compare patients with nonsevere disease, survivors with severe disease, and nonsurvivors with severe disease and are calculated from the Kruskall-Wallis test.

ease at admission, 38.6% (27/70) were admitted or transferred to an ICU, 21.4% (15/70) died, and 78.6% (55/70) recovered and were discharged. The survivors with severe disease and the nonsurvivors were both significantly older (median age, 53.0 years [IQR, 39.0–62.5 years] and 72.0 years [IQR, 64.5–74.5 years], respectively) than the survivors with nonsevere disease (median age, 37.0 years [IQR, 30.5–45.5 years]; $p < .001$). The survivors with severe disease and nonsurvivors were also more likely to have underlying comorbidities (40.0% [22/55] and 86.7% [13/15], respectively) compared with survivors with nonsevere disease (15.4% [14/91]; $p < .001$). The nonsurvivors had significantly higher systolic blood pressure ($p = .004$) and respiratory rate ($p < .001$) on admission compared with the other two groups.

Table 2 shows the laboratory findings on admission. Lymphocytopenia (lymphocyte count < 1.5 × 10^9/L) was present in 88.2% of the cohort, leukopenia (WBC count < 4.0 × 10^9/L) in 40.4%, and thrombocytopenia (platelet count < 150 × 10^9/L) in 37.3%. WBC count, neutrophil count, D-dimer, aspartate aminotransferase, total bilirubin, blood urea nitrogen, creatinine, creatine kinase myocardial band, lactate dehydrogenase, and high-sensitivity troponin were significantly different among the three groups, showing progressive increases from survivors with nonsevere disease to survivors with severe disease to nonsurvivors ($p < .05$).

Longitudinal CT Findings

All patients showed abnormal CT findings during the course of their disease (Table 3). The median CT visual lung severity score in the first week of hospitalization was 2.0 in survivors with nonsevere disease, 4.0 in survivors with severe disease, and 11.0 in nonsurvivors. In week 1, a peripheral distribution was observed in 83.1% survivors with nonsevere disease, 73.7% of survivors with severe disease, and 11.1% of nonsurvivors. A total of 36.1% of survivors with nonsevere disease had three or more lobes affected compared with 65.8% of survivors with severe disease and 100.0% of nonsurvivors. GGO without consolidation was the most common pattern for all three groups (76.3–88.9%); in comparison,

TABLE 3: Distribution and Frequency of Lung Lesions on CT at Different Time Stages by Disease Severity

Lung Lesion Characteristic	Week 1			Week 2			Week 3		Week 4 or Later	
	Survivors, Nonsevere (*n* = 83)	Survivors, Severe (*n* = 38)	Nonsurvivors (*n* = 9)	Survivors, Nonsevere (*n* = 78)	Survivors, Severe (*n* = 50)	Nonsurvivors (*n* = 9)	Survivors, Nonsevere (*n* = 49)	Survivors, Severe (*n* = 36)	Survivors, Nonsevere (*n* = 40)	Survivors, Severe (*n* = 24)
GGOs and consolidation										
Normal	5 (6.0)	2 (5.3)	0 (0)	2 (2.6)	0 (0)	0 (0)	9 (18.4)	3 (8.3)	16 (40.0)	3 (12.5)
GGOs only	64 (77.1)	29 (76.3)	8 (88.9)	54 (69.2)	27 (54.0)	5 (55.6)	23 (46.9)	14 (38.9)	20 (50.0)	8 (33.3)
Consolidation only	2 (2.4)	0 (0)	0 (0)	2 (2.6)	0 (0)	0 (0)	6 (12.2)	2 (5.6)	3 (7.5)	3 (12.5)
Both	12 (14.5)	7 (18.4)	1 (11.1)	20 (25.6)	23 (46.0)	4 (44.4)	11 (22.4)	17 (47.2)	1 (2.5)	10 (41.7)
Lobes involved										
RUL	26 (31.3)	24 (63.2)	7 (77.8)	32 (41.0)	44 (88.0)	8 (88.9)	18 (36.7)	29 (80.6)	7 (17.5)	20 (83.3)
RML	25 (30.1)	21 (55.3)	7 (77.8)	25 (32.1)	39 (78.0)	8 (88.9)	15 (30.6)	27 (75.0)	8 (20.0)	17 (70.8)
RLL	59 (71.1)	27 (71.1)	8 (88.9)	61 (78.2)	45 (90.0)	8 (88.9)	35 (71.4)	30 (83.3)	21 (52.5)	21 (87.5)
LUL	30 (36.1)	23 (60.5)	8 (88.9)	37 (47.4)	43 (86.0)	6 (66.7)	20 (40.8)	28 (77.8)	12 (30.0)	20 (83.3)
LLL	48 (57.8)	31 (81.6)	8 (88.9)	56 (71.8)	47 (94.0)	8 (88.9)	34 (69.4)	34 (94.4)	22 (55.0)	22 (91.7)
No. of lobes affected										
0	6 (7.2)	2 (5.3)	0 (0)	2 (2.6)	0 (0)	0 (0)	9 (18.4)	1 (2.8)	14 (35.0)	2 (8.3)
1	27 (32.5)	8 (21.1)	0 (0)	17 (21.8)	3 (6.0)	0 (0)	8 (16.3)	2 (5.6)	5 (12.5)	0 (0)
2	20 (24.1)	3 (7.9)	0 (0)	20 (25.6)	2 (4.0)	0 (0)	9 (18.4)	1 (2.8)	8 (20.0)	0 (0)
3	9 (10.8)	4 (10.5)	1 (11.1)	15 (19.2)	3 (6.0)	0 (0)	6 (12.2)	4 (11.1)	6 (15.0)	3 (12.5)
4	10 (12.0)	5 (13.2)	0 (0)	10 (12.8)	8 (16.0)	2 (22.2)	7 (14.3)	8 (22.2)	4 (10.0)	4 (16.7)
5	11 (13.3)	16 (42.1)	8 (88.9)	14 (17.9)	34 (68.0)	7 (77.8)	10 (20.4)	20 (55.6)	3 (7.5)	15 (62.5)
Bilateral lung disease										
None	6 (7.2)	2 (5.3)	0 (0)	2 (2.6)	0 (0)	0 (0)	9 (18.4)	1 (2.8)	14 (35.0)	2 (8.3)
One side	29 (34.9)	9 (23.7)	1 (11.1)	19 (24.4)	3 (6.0)	0 (0)	8 (16.3)	2 (5.6)	6 (15.0)	0 (0)
Both sides	48 (57.8)	27 (71.1)	8 (88.9)	57 (73.1)	47 (94.0)	9 (100.0)	32 (65.3)	33 (91.7)	20 (50.0)	22 (91.7)
Opacification distribution and pattern										
Peripheral distribution	69 (83.1)	28 (73.7)	1 (11.1)	72 (92.3)	29 (58.0)	2 (22.2)	39 (79.6)	27 (75.0)	25 (62.5)	19 (79.2)
Linear opacities	3 (3.6)	2 (5.3)	0 (0)	16 (20.5)	8 (16.0)	0 (0)	19 (38.8)	17 (47.2)	11 (27.5)	17 (70.8)
Crazy paving pattern	2 (2.4)	1 (2.6)	5 (55.6)	2 (2.6)	9 (18.0)	4 (44.4)	0 (0)	8 (22.2)	0 (0)	1 (4.2)
Total lung severity score										
Median	2.0	4.0	11.0	3.0	8.0	12.0	3.0	6.0	2.0	5.0
IQR	1.0–4.0	1.3–7.0	9.0–12.0	2.0–5.0	5.0–10.0	10.0–13.0	1.0–4.0	4.0–7.3	0.0–3.0	4.8–6.0

Note—Data are the number of patients (percentage) unless otherwise indicated. GGO = ground-glass opacity, RUL = right upper lobe, RML = right middle lobe, RLL = right lower lobe, LUL = left upper lobe, LLL = left lower lobe, IQR = interquartile range.

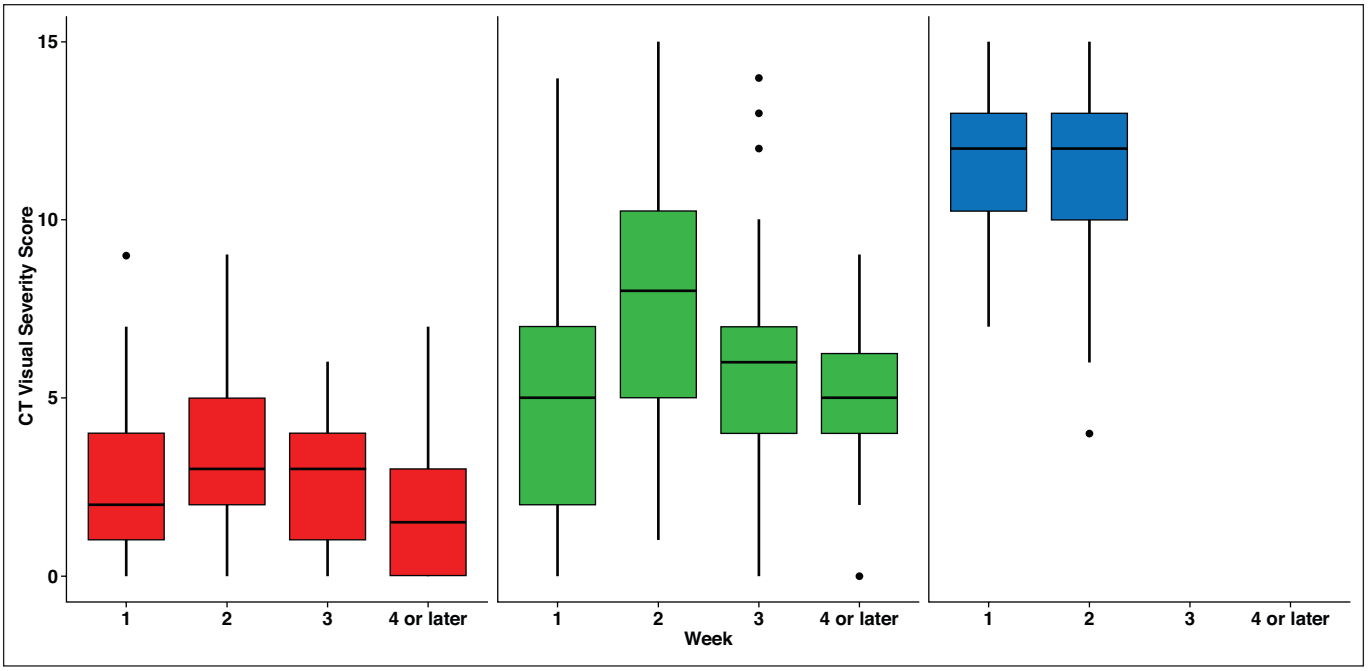

Fig. 1—Box-and-whisker plots show CT visual severity scores by time interval for survivors with nonsevere coronavirus disease (COVID-19) (*left, red*), survivors with severe disease (*middle, green*), and patients who did not survive (*right, blue*). Upper and lower limits of whiskers indicate represent 1.5 times interquartile range above and below upper and lower quartiles, respectively, and dots indicate outliers.

11.1–18.4% had GGO with consolidation in week 1. In week 2, 73.1–100.0% had bilateral lung involvement and 25.6–46.0% had GGO with consolidation. These percentages of patients showing GGO with consolidation were similar in week 3. In week 4, 2.5% of survivors with nonsevere disease and 41.7% of survivors with severe disease showed GGO with consolidation.

Figure 1 displays the temporal evolution of CT visual severity scores according to disease severity. For survivors with both nonsevere and severe disease, the CT visual severity score reached a peak in week 2 after symptom onset and then decreased progressively in weeks 3 and 4. Nonsurvivors showed much higher CT visual severity scores compared with survivors and no visually apparent decrease between weeks 1 and 2. Figure 2 displays the regression curve fits for survivors with nonsevere and severe disease. The two curves were not parallel ($p < .001$), indicating different disease evolution patterns between the two groups. Change point detection analysis showed that the peak CT visual severity score for survivors with nonsevere disease on admission was reached approximatelyf 9 days (95% CI, 7–11) from symptom onset, whereas the peak score for survivors with severe disease was reached approximately 12 days (95% CI, 11–14) from symptom onset.

Representative serial CT images from patients with nonsevere and severe disease are shown in Figures S1 and S2, respectively, which can be viewed in the *AJR* electronic supplement to this article, available at www.ajronline.org.

Risk Factors Associated With the Composite Complications and a Prognostic Model

A total of 77.0% of patients (124/161) had no complications of COVID-19, and 23.0% (37/161) had at least one complication. Complications included ARDS (20.5%), AKI (7.5%), liver dysfunction (6.8%), acute cardiac injury (6.8%), septic shock (6.2%), arrhythmia (5.6%), and secondary infection (3.1%) (Table S1, which can be viewed in the *AJR* electronic supplement to this article, available at www.ajronline.org). All complications were significantly more common ($p < .001$) in patients with severe disease. In univariable logistic regression analysis (Table 4), age, sex, respiratory rate, neutrophil count, lymphocyte count, procalcitonin, D-dimer levels over 1 mg/L, alanine aminotransferase, creatinine, lactate dehydrogenase, and the first CT severity score following admission were all associated with the composite complication endpoint ($p < .05$).

The multivariable model for predicting in-hospital complications was constructed using the following four variables: age, sex, lymphocyte count, and the first CT visual severity score after admission (Table 4). In the model, the factor with the highest odds for predicting in-hospital complications was the CT visual severity score (odds ratio, 5.86 [95% CI, 1.70–20.23] for moderate score [$p = .005$] and 31.28 [95% CI, 2.97–329.80] for severe score [$p = .004$]). Complications were also significantly associated with older age (odds ratio, 1.09 [95% CI, 1.09–1.14] per 1-year increase; $p < .001$) and lower lymphocyte count (odds ratio, 0.03 [95% CI, 0.00–0.29] per 1×10^9/L increase; $p = .002$). Sex was not a significant independent predictor in this model ($p = .45$).

Internal and External Model Validations

The internal bootstrap validation of the model for predicting in-hospital complications showed a bias-corrected C-index of 0.94 (Fig. S3, which can be viewed in the *AJR* electronic supplement to this article, available at www.ajronline.org). In the calibration plot (Fig. S4, also available in the *AJR* electronic supplement to this article at www.ajronline.org), predicted probabilities closely matched the actual probabilities, indicating that the model performed reasonably well. Although slight underprediction

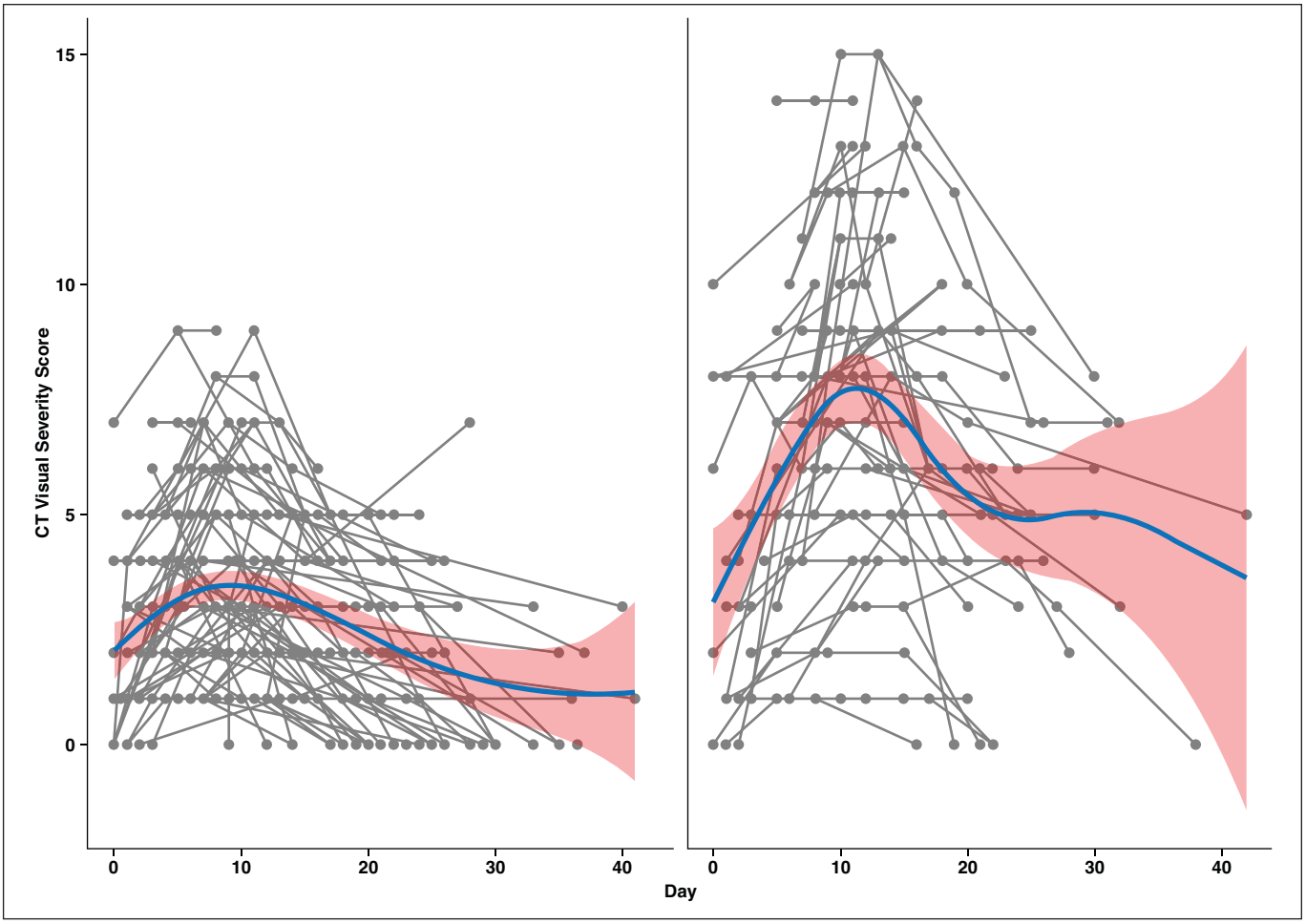

Fig. 2—Nonlinear regression curve fits with 95% CIs. Graphs show lung CT visual severity scores for survivors with nonsevere coronavirus disease (COVID-19) (*left*) and survivors with severe disease (*right*). Peak CT score occurred approximately 9 days from symptom onset (95% CI, 7–11 days) for patients with nonsevere disease compared with 12 days (95% CI, 11–14 days) for survivors with severe disease. Gray dots and lines represent CT visual severity scores for individual patients; curved blue lines and shaded areas represent estimated mean functions and 95% CIs, respectively.

or overprediction occurred at lower predicted probabilities (< .5), the prediction was highly accurate at higher predicted probabilities (≥ .5).

Tables S2–S4 (which can be viewed in the *AJR* electronic supplement to this article, available at www.ajronline.org) present the demographic, laboratory, and outcome variables, respectively, for the 135 patients in the external validation cohort from a different hospital. The median age was 53.0 years (IQR, 38.0–66.0 years). This cohort included 70 (51.9%) men and 65 (48.1%) women. The weighted kappa interreader agreement between the two readers for the CT-based visual severity level was 0.83 (95% CI, 0.73–0.92).

In the external validation cohort, the prediction model showed a C-index of 0.95 and 0.92 using the CT visual severity scores from the two readers (Fig. S5, which can be viewed in the *AJR* electronic supplement to this article, available at www.ajronline.org). When using $p \geq .5$ as the cut point for predicting complications on the basis of the CT scores, reader 1 achieved an accuracy of 86.7%, sensitivity of 75.6%, and specificity of 91.5%, whereas reader 2 achieved an accuracy of 85.2%, sensitivity of 70.7%, and specificity of 91.4%.

Discussion

We found that a CT visual severity score is associated with patients' clinical disease severity and shows characteristic temporal changes over the course of disease progression after hospital admission. Further, the CT visual severity score in combination with several clinical variables on admission accurately predicts in-hospital complications in patients with COVID-19.

This study cohort is representative of patients who acquired COVID-19 and required hospitalization in Hubei, China. We built the prediction model using data from serial CT scans and the complete medical records for 161 patients with SARS-CoV-2 pneumonia. We then performed model validation using admission CT and clinical information for an independent sample of 135 patients.

The CT visual severity score may assist with the diagnosis and treatment of patients with COVID-19. Serial CT scans could monitor the progression or improvement of lung lesions during treatment, which dynamically reflects therapeutic effects. For example, we identified different temporal patterns for this score between patients with nonsevere disease and survivors with severe disease (peak scores occurring at at approximately 9 vs 12

TABLE 4: Risk Factors Associated With the In-Hospital Composite Endpoint

Variable	Univariable		Multivariable	
	Odds Ratio (95% CI)	*p*	Odds Ratio (95% CI)	*p*
Age (y)	1.12 (1.08–1.17)	< .001	1.09 (1.04–1.14)	< .001
Sex (reference: female)				
Male	2.29 (1.04–5.03)	.04	1.58 (0.48–5.20)	.45
Respiratory rate (breaths/min)	1.31 (1.12–1.54)	.001		
WBC count (× 10^9/L; reference: ≥ 4)				
< 4	0.73 (0.34–1.56)	.41		
Neutrophil count (× 10^9/L)	1.60 (1.27–2.02)	< .001		
Lymphocyte count (× 10^9/L)	0.01 (0.00–0.07)	< .001	0.03 (0.00–0.29)	.002
Monocyte count (× 10^9/L)	0.49 (0.08–3.00)	.44		
Platelet count (× 10^9/L; reference: ≥ 150)				
< 150	1.39 (0.66–2.93)	.39		
Procalcitonin (ng/mL; reference: < 0.05)				
≥ 0.05	3.72 (1.73–8.00)	.001		
D-Dimer (mg/L; reference: < 0.5)				
0.5–1	1.58 (0.45–5.52)	.55		
> 1	5.96 (2.10–16.94)	.001		
Alanine aminotransferase (U/L)	1.01 (1.00–1.02)	.03		
Creatinine (μmol/L)	1.05 (1.02–1.07)	< .001		
Lactate dehydrogenase (U/L)	1.01 (1.01–1.02)	< .001		
CT severity score[a] (reference: score ≤ 5)				
Moderate (6–10)	13.24 (4.89–35.85)	< .001	5.86 (1.70–20.23)	.005
Severe (> 10)	176.57 (19.98–1560.37)	< .001	31.28 (2.97–329.80)	.004

[a]First CT visual severity score after admission.

days, respectively). Compared with the studies by Shi et al. [7] and Wang et al. [9], our findings provide better insights into the association of the evolution of CT findings with clinical disease severity. In survivors with nonsevere disease, chest CT abnormalities worsened in approximately the first 9 days and then gradually improved. In survivors with severe disease, the peak was reached in approximately 12 days. Thus, a poor prognosis should be expected if chest CT findings do not show improvement within approximately 2 weeks of initial symptoms.

We developed a prognostic model to predict major complications or death using four readily-obtained factors: age, sex, lymphocyte count, and CT visual severity level. We selected these factors on the basis of the following considerations: possible unavailability of more complex laboratory values on admission, previous research findings [4, 5, 8, 25], and ease of use of the model. CT visual severity level was stratified as less than 50%, 50–75%, and more than 75% pulmonary involvement. Radiologists can easily provide this classification by reviewing an admission chest CT scan. A review by Wynants et al. [26] found that many prediction models for COVID-19 are poorly reported and at high risk of bias. Nonetheless, our model, which is publicly available online [24], followed the TRIPOD guidelines and showed high discrimination on both internal and external validations.

Our study has some limitations. First, because of the retrospective study design, we evaluated patients who underwent serial CT scans, which were not based on a predefined protocol but were ordered based on clinical need. This design introduces a selection bias. The included patients were admitted to hospitals between January 10, 2020, and February 7, 2020, during the early period of the COVID-19 epidemic in Hubei. During this time period, there was a limited supply of medical resources, such as hospital beds, ICU beds, and ventilators. Moreover, the mortality rate in our cohort was higher than the global estimate. Patients recovering more quickly were likely to undergo fewer serial CT scans. Therefore, the estimate of the peak CT severity applies only to patients ill enough to undergo serial imaging. Second, the sample size is limited. Third, serial laboratory tests were not obtained in all patients, precluding our ability to create a dynamic prediction model. Fourth, we did not assess the impact of the use of different CT scanners.

Conclusion

A CT visual severity score is associated with patients' clinical disease severity and evolves in a characteristic fashion over the course of hospitalization. A prognostic model based on the CT visual severity score and readily available clinical variables shows

strong performance in predicting in-hospital complications. This prognostic model may help identify patients at highest risk of poor outcomes and guide early intervention.

References

1. WHO website. Clinical management of severe acute respiratory infection when novel coronavirus (2019-nCoV) infection is suspected: interim guidance, 28 January 2020. apps.who.int/iris/handle/10665/330893. Accessed August 6, 2020
2. Huang C, Wang Y, Li X, et al. Clinical features of patients infected with 2019 novel coronavirus in Wuhan, China. *Lancet* 2020; 395:497–506
3. Chen N, Zhou M, Dong X, et al. Epidemiological and clinical characteristics of 99 cases of 2019 novel coronavirus pneumonia in Wuhan, China: a descriptive study. *Lancet* 2020; 395:507–513
4. Wang D, Hu B, Hu C, et al. Clinical characteristics of 138 hospitalized patients with 2019 novel coronavirus-infected pneumonia in Wuhan, China. *JAMA* 2020; 323:1061–1069
5. Guan WJ, Ni ZY, Hu Y, et al.; China Medical Treatment Expert Group for Covid-19. Clinical characteristics of coronavirus disease 2019 in China. *N Engl J Med* 2020; 382:1708–1720
6. Chung M, Bernheim A, Mei X, et al. CT imaging features of 2019 novel coronavirus (2019-nCoV). *Radiology* 2020; 295:202–207
7. Shi H, Han X, Jiang N, et al. Radiological findings from 81 patients with COVID-19 pneumonia in Wuhan, China: a descriptive study. *Lancet Infect Dis* 2020; 20:425–434
8. Pan F, Ye T, Sun P, et al. Time course of lung changes at chest CT during recovery from coronavirus disease 2019 (COVID-19). *Radiology* 2020; 295:715–721
9. Wang Y, Dong C, Hu Y, et al. Temporal changes of CT findings in 90 patients with COVID-19 pneumonia: a longitudinal study. *Radiology* 2020; 296:E55–E64
10. Jin YH, Cai L, Cheng ZS, et al.; Zhongnan Hospital of Wuhan University Novel Coronavirus Management and Research Team, Evidence-Based Medicine Chapter of China International Exchange and Promotive Association for Medical and Health Care (CPAM). A rapid advice guideline for the diagnosis and treatment of 2019 novel coronavirus (2019-nCoV) infected pneumonia (standard version). *Mil Med Res* 2020; 7:4
11. Zhang G, Hu C, Luo L, et al. Clinical features and short-term outcomes of 221 patients with COVID-19 in Wuhan, China. *J Clin Virol* 2020; 127:104364
12. International Severe Acute Respiratory and Emerging Infection Consortium. Severe acute respiratory infection data tools. isaric.tghn.org/protocols/severe-acute-respiratory-infection-data-tools/. Accessed August 6, 2020
13. Metlay JP, Waterer GW, Long AC, et al. Diagnosis and treatment of adults with community-acquired pneumonia: an official clinical practice guideline of the American Thoracic Society and Infectious Diseases Society of America. *Am J Respir Crit Care Med* 2019; 200:e45–e67
14. Ranieri VM, Rubenfeld GD, Thompson BT, et al.; ARDS Definition Task Force. Acute respiratory distress syndrome: the Berlin definition. *JAMA* 2012; 307:2526–2533
15. Khwaja A. KDIGO clinical practice guidelines for acute kidney injury. *Nephron Clin Pract* 2012; 120:c179–c184
16. Singer M, Deutschman CS, Seymour CW, et al. The third international consensus definitions for sepsis and septic shock (sepsis-3). *JAMA* 2016; 315:801–810
17. Zhang C, Shi L, Wang FS. Liver injury in COVID-19: management and challenges. *Lancet Gastroenterol Hepatol* 2020; 5:428–430
18. Xu L, Liu J, Lu M, Yang D, Zheng X. Liver injury during highly pathogenic human coronavirus infections. *Liver Int* 2020; 40:998–1004
19. Wood SN. *Generalized additive models: an introduction with R*. CRC Press, 2017
20. Dette H, Neumeyer N. Nonparametric analysis of covariance. *Ann Stat* 2001; 29:1361–1400
21. Gijbels I, Goderniaux AC. Bootstrap test for change-points in nonparametric regression. *J Nonparametr Stat* 2004; 16:591–611
22. Moons KG, Altman DG, Reitsma JB, et al. Transparent Reporting of a multivariable prediction model for Individual Prognosis or Diagnosis (TRIPOD): explanation and elaboration. *Ann Intern Med* 2015; 162:W1–W73
23. Steyerberg EW, Harrell FE Jr, Borsboom GJJM, Eijkemans MJC, Vergouwe Y, Habbema JDF. Internal validation of predictive models: efficiency of some procedures for logistic regression analysis. *J Clin Epidemiol* 2001; 54:774–781
24. Cleveland Clinic. Predict probability of having complications for patients with covid-19. riskcalc.org/covid-19-complications/. Accessed August 6, 2020
25. Zhou F, Yu T, Du R, et al. Clinical course and risk factors for mortality of adult inpatients with COVID-19 in Wuhan, China: a retrospective cohort study. *Lancet* 2020; 395:1054–1062
26. Wynants L, Van Calster B, Collins GS, et al. Prediction models for diagnosis and prognosis of COVID-19 infection: systematic review and critical appraisal. *BMJ* 2020; 369:m1328

Editorial Comment on "Multicenter Study of Temporal Changes and Prognostic Value of a CT Visual Severity Score in Hospitalized Patients With Coronavirus Disease (COVID-19)"

The authors analyzed the clinical course and CT findings of a cohort of patients from three hospitals in Hubei Province and developed a model to predict in-hospital complications. Importantly, this model was then validated using a separate cohort of patients from a fourth hospital. Use of separate datasets to validate predictive models is often neglected in the radiology literature, and failure to do so results in falsely high sensitivity, specificity, and accuracy of the proposed model.

How might this validated model be of use to referring clinicians and radiologists? The latest WHO guidelines highlight the lack of available evidence to guide the use of imaging in the treatment of patients with COVID-19 [1]. As existing potential therapies are developed and new therapies are introduced, determining at what stage and at what level of clinical severity these therapies are best used will be important. The apparent significant prognostic value of the severity of CT abnormalities may prove valuable in guiding the use of candidate therapies in clinical trials and in selecting the patient populations most likely to benefit.

If CT does prove useful in guiding therapy, the authors' CT severity index is simple to calculate and could easily be incorporated into a radiology report. Moreover, the authors and the Cleveland Clinic have provided an online calculator based on their model [2]. This model contains four input variables: the CT severity score as described in the article and the patient's sex, age, and lymphocyte count.

Michael A. Brooks, MD
Virginia Tech Carilion School of Medicine
Roanoke, VA
mbrooks1@carilionclinic.org

The author declares that there are no disclosures relevant to the subject matter of this article.

doi.org/10.2214/AJR.20.24644

References

1. Akl EA, Blazic I, Yaacoub S, et al. Use of chest imaging in the diagnosis and management of COVID-19: a WHO rapid advice guide. *Radiology* 2020 Jul 30 [published online]
2. Cleveland Clinic. Predict probability of having complications for patients with covid-19. riskcalc.org/covid-19-complications/. Accessed August 21, 2020